CrossMark

J. Fluid Mech. (2015), *vol.* 778, *pp.* 669–690. © Cambridge University Press 2015
doi:10.1017/jfm.2015.406

Converging gravity currents over a permeable substrate

Zhong Zheng[1], **Sangwoo Shin**[1] **and Howard A. Stone**[1,†]

[1]Department of Mechanical and Aerospace Engineering, Princeton University, Princeton, NJ 08544, USA

(Received 19 January 2015; revised 10 July 2015; accepted 12 July 2015; first published online 7 August 2015)

We study the propagation of viscous gravity currents along a thin permeable substrate where slow vertical drainage is allowed from the boundary. In particular, we report the effect of this vertical fluid drainage on the second-kind self-similar solutions for the shape of the fluid–fluid interface in three contexts: (i) viscous axisymmetric gravity currents converging towards the centre of a cylindrical container; (ii) viscous gravity currents moving towards the origin in a horizontal Hele-Shaw channel with a power-law varying gap thickness in the horizontal direction; and (iii) viscous gravity currents propagating towards the origin of a porous medium with horizontal permeability and porosity gradients in power-law forms. For each of these cases with vertical leakage, we identify a regime diagram that characterizes whether the front reaches the origin or not; in particular, when the front does not reach the origin, we calculate the final location of the front. We have also conducted laboratory experiments with a cylindrical lock gate to generate a converging viscous gravity current where vertical fluid drainage is allowed from various perforated horizontal substrates. The time-dependent position of the propagating front is captured from the experiments, and the front position is found to agree well with the theoretical and numerical predictions when surface tension effects can be neglected.

Key words: geophysical and geological flows, gravity currents, thin films

1. Introduction

The spreading of viscous gravity currents arises in many geophysical and industrial contexts, and has received renewed attention as a result of technical challenges posed by geological CO_2 sequestration and other subsurface fluid mechanics problems (see e.g. Bear 1972; Barenblatt 1979; Lake 1989; Nordbotten & Celia 2012; Huppert & Neufeld 2014). The analysis of many of these problems proceeds using the lubrication approximation to reduce the flow problem to a single nonlinear partial differential equation (PDE) for the shape of the spreading current. The time-dependent extent of spreading is also an output of the solution to the problem. In standard cases involving outward spreading, the solution to the PDE can be accomplished by dimensional inspection; such first-kind similarity solutions have been presented for many geometries: lock exchange, spreading over substrates and through porous media,

†Email address for correspondence: hastone@princeton.edu

https://doi.org/10.1017/jfm.2015.406 Published online by Cambridge University Press

or other confined systems, etc. (see e.g. Smith 1969; Huppert 1982; Lister 1992; Huppert & Woods 1995; Nordbotten & Celia 2006; Hesse *et al.* 2007; MacMinn, Szulczewski & Juanes 2010; Pegler, Huppert & Neufeld 2014*a*; Zheng *et al.* 2015).

Many natural systems leak either through an edge or through a fractured or porous boundary. Also, various coating flows occur above porous substrates. Because the boundaries are porous, a variety of studies in recent years have analysed spreading gravity currents with leakage (Acton, Huppert & Worster 2001; Pritchard, Woods & Hogg 2001; Pritchard & Hogg 2002; Pritchard 2007; Neufeld & Huppert 2009; Neufeld, Vella & Huppert 2009; Spannuth *et al.* 2009; Neufeld *et al.* 2011; Vella *et al.* 2011; Zemoch, Neufeld & Vella 2011; Zheng *et al.* 2013). In this case, it is possible in some cases involving outward spreading to make a change of variables to arrive back at a PDE that again admits a similarity solution of the first kind (Pritchard *et al.* 2001). A brief summary of previous studies on fluid drainage effects on the 'outward' propagation of viscous gravity currents is provided in table 1

A distinct class of thin film spreading problems concerns 'inward' motions, where the reservoir or source of fluid is on the outside and motion occurs towards an 'origin' (Gratton & Minotti 1990; Diez, Gratton & Gratton 1992; Zheng, Christov & Stone 2014). In these cases, although the same PDE describes the dynamics, a first-kind similarity solution is not possible. Rather, given a scaling ansatz, a distinct analysis of the differential equations for mass and momentum is used to construct an eigenvalue style analysis to determine the scaling exponent (Barenblatt 1979). In this paper, we present such an analysis for converging spreading gravity currents with leakage through a thin permeable boundary (figure 1), which to the best of our knowledge has not been treated previously. We highlight the general idea and so summarize how the approach and results apply to various geometric configurations. In addition, our experimental set-up of fluid drainage through a thin perforated plate (§ 3) provides a new model experimental system to study the behaviour of fluid drainage from spreading gravity currents, and extends the existing experimental systems of drainage through a deep porous medium (Acton *et al.* 2001), through long parallel tubes (Spannuth *et al.* 2009) and through thin parallel plates (Pritchard *et al.* 2001).

In structuring this paper, we begin in § 2 by studying the model problem of a converging viscous gravity current with fluid drainage in the axisymmetric geometry; we describe the theoretical model, introduce a transformation of variables and derive a second-kind self-similar solution considering the effect of vertical fluid drainage. In § 3, we conduct laboratory-scale experiments, and compare the experimental observations with the predictions of our theoretical models. We extend our discussion in § 4 to viscous gravity currents in Hele-Shaw cells and porous media with horizontal heterogeneities and leakage so as to characterize similar problems as broadly as possible. We close our paper in § 5 with some final remarks.

2. Theoretical model

2.1. *Governing equations*

We consider an axisymmetric geometry and describe the thin film flow using cylindrical coordinates. In particular, we first examine the inward spreading of a converging gravity current on a permeable boundary of thickness d and permeability k_d, see figure 2. The viscosity of the fluid is μ, and the density of the fluid is $\rho_a + \Delta\rho$, where ρ_a is the density of air. The height of the air–liquid interface is denoted as $h(r, t)$. We neglect the effect of surface tension and fluid mixing at the

https://doi.org/10.1017/jfm.2015.406 Published online by Cambridge University Press

Reservoir condition	Substrate description	Experiment[a]	Reference
Exposed in air, two-dimensional	Deep porous medium	Yes	Acton *et al.* (2001)
Exposed in air, axisymmetric	Parallel vertical tubes	Yes	Spannuth *et al.* (2009)
Porous media	Thin permeable layer	Yes	Pritchard *et al.* (2001)
Porous media, two-dimensional	Vertical fracture	No	Pritchard & Hogg (2002)
Porous media, two-dimensional	Parallel fractures	No	Pritchard (2007)
Porous media, two-dimensional	Thin permeable layer	No	Neufeld & Huppert (2009)
Porous media, two-dimensional	Permeable layer, (capillary retention)	No	Farcas & Woods (2009)
Porous media, two-dimensional	Permeable layer, (capillary threshold)	No	Woods & Farcas (2009)
Porous media, two-dimensional	Local fissure	Yes	Neufeld *et al.* (2009)
Porous media, two-dimensional	Local fissure, (inclined substrate)	No	Zemoch *et al.* (2011)
Porous media, point injection	Local point sink	No	Neufeld *et al.* (2011)
Porous media, point injection	Local line sink	No	Vella *et al.* (2011)
Porous media, two-dimensional	Multiple fractures, (multiple layers)	Yes	Hesse & Woods (2010)
Porous media, two-dimensional	Drainage from edge	Yes	Zheng *et al.* (2013)
Porous media, confined layers	Local point sink (and multiple sinks)	No	Nordbotten *et al.* (2009)
Porous media, confined layers	Local fissure	No	Pegler, Huppert & Neufeld (2014*b*)
Exposed in air, axisymmetric	Thin permeable layer (inward flow)	Yes	Current work
Heterogeneous, porous media, Hele-Shaw cells	Thin permeable layer (flow towards 'origin')	No	Current work

TABLE 1. Summary of previous studies on the propagation of a viscous gravity current over a permeable substrate such that vertical fluid drainage occurs through the substrate. All of the references except for the last two referring to this paper concern outward spreading and so similarity solutions of the first kind are possible. In the current work, for propagation of gravity currents in Hele-Shaw cells and porous media with horizontal heterogeneities, the 'origin' is defined as the location of zero permeability.

[a]We note that in the current study and some previous studies experiments have also been conducted to verify the theoretical models.

https://doi.org/10.1017/jfm.2015.406 Published online by Cambridge University Press

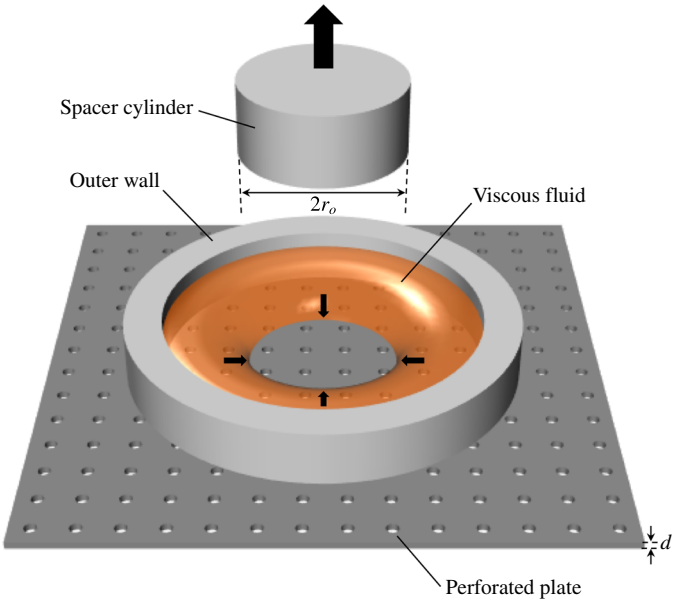

FIGURE 1. (Colour online) Schematic of a converging gravity current on a thin permeable plate with fluid drainage through the substrate in the vertical direction. Initially, a viscous fluid fills the space between the outer wall and a spacer cylinder. Then, the inward flow is initiated by removing the spacer cylinder, i.e. the flow is due to a 'cylindrical lock gate'. For the finer spacing of holes used in the experiments, see figure 4.

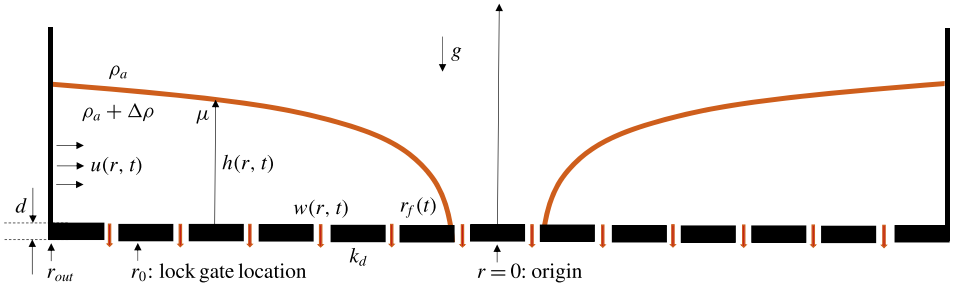

FIGURE 2. (Colour online) Side view of an axisymmetric converging gravity current on a thin permeable plate with thickness d and permeability k_d. Slow fluid drainage occurs in the vertical direction through the substrate. Flow is generated by removing a cylindrical lock gate (not shown), which is located at r_0 (figure 1).

interface and contact line effects at the moving boundary, as well as viscous stresses at the air–liquid boundary. When the spreading current is long and thin, it is natural to use the lubrication approximation, in which case we neglect the vertical velocity and the fluid has a hydrostatic pressure distribution. Following standard steps, the vertically averaged velocity along the horizontal direction $u(r, t)$ is given by

$$u(r, t) = -\frac{\Delta\rho g h^2}{3\mu}\frac{\partial h}{\partial r}. \tag{2.1}$$

https://doi.org/10.1017/jfm.2015.406 Published online by Cambridge University Press

Next, we assume that the thickness of the permeable boundary d is small compared with the height of the gravity current h, i.e. $h/d \gg 1$; this assumption is only violated in a region very close to the front. Since fluid is allowed to drain from the permeable boundary, the gravitationally driven drainage rate $w(r, t)$ $(w < 0)$ is estimated by

$$w(r, t) = -\frac{\Delta\rho g k_d}{\mu}\left(1 + \frac{h}{d}\right) \approx -\frac{\Delta\rho g k_d h}{\mu d}, \tag{2.2}$$

where k_d is the effective permeability of the substrate. This model has been employed in several previous studies on the spreading of gravity currents with vertical fluid drainage (see e.g. Acton *et al.* 2001; Pritchard *et al.* 2001; Pritchard & Hogg 2002; Pritchard 2007; Spannuth *et al.* 2009; Neufeld *et al.* 2011; Vella *et al.* 2011). The applicability of this model has been discussed in other viscous film spreading problems on porous bases (see e.g. Davis & Hocking 1999, 2000). Note that if the permeable boundary is a perforated plate, e.g. as in our laboratory experiments presented below, when estimating k_d, the resistance from entering and exiting the holes may also need to be considered if the thickness of the plate is small (see e.g. Sampson 1891; Weissberg 1962; Dagan, Weinbaum & Pfeffer 1982; Jensen, Valente & Stone 2014).

Considering fluid drainage, the local continuity equation is written as

$$\frac{\partial h}{\partial t} + \frac{1}{r}\frac{\partial}{\partial r}(rhu) = w, \tag{2.3}$$

where the drainage rate w is given by (2.2). Substituting (2.1) and (2.2) into (2.3), we obtain a PDE that describes the time evolution of the air–liquid interface:

$$\frac{\partial h}{\partial t} - \frac{\Delta\rho g}{3\mu}\frac{1}{r}\frac{\partial}{\partial r}\left(rh^3\frac{\partial h}{\partial r}\right) = -\frac{\Delta\rho g k_d h}{\mu d}. \tag{2.4}$$

Note that in previous studies on outward-spreading viscous gravity currents over permeable substrates, the governing equations for the fluid–fluid interface are the same as or similar to (2.4) (see e.g. Acton *et al.* 2001; Pritchard *et al.* 2001; Spannuth *et al.* 2009). However, converging currents are distinguished by distinct boundary conditions, and a different solution procedure also needs to be described, as given below.

To complete the problem, appropriate boundary and initial conditions are needed. We assume that a viscous fluid of height h_0 initially fills the space between $r = r_0$, i.e. the location of the cylindrical lock gate, and $r = r_{out}$, i.e. the radius of a cylindrical tank. Thus, the initial condition is given by

$$h(r, 0) = \begin{cases} h_0, & r_0 \leqslant r < r_{out}, \\ 0, & 0 \leqslant r < r_0. \end{cases} \tag{2.5}$$

The boundary conditions for this problem are given by

$$\frac{\partial h}{\partial r}(r_{out}, t) = 0, \tag{2.6a}$$

$$h(r_f(t), t) = 0, \tag{2.6b}$$

where $r_f(t)$ denotes the location of the moving front. In order to develop second-kind similarity solutions, where dimensional inspection is not sufficient to determine the functional form of $r_f(t)$, it is necessary to consider the momentum (2.1) and continuity (2.3) equations in their primitive forms. Our main goal is to describe the propagation of the fluid towards $r \to 0$, i.e. to determine $r_f(t)$ for $k_d \neq 0$. Note that when $k_d = 0$, i.e. when the substrate is not permeable, the problem statement reduces to the previous

https://doi.org/10.1017/jfm.2015.406 Published online by Cambridge University Press

studies of second-kind similarity solutions given by Gratton & Minotti (1990) and Diez *et al.* (1992).

2.2. *Non-dimensionalization*

Let us now define dimensionless variables $\tilde{h} = h/h_0$, $\tilde{r} = r/r_0$, $\tilde{t} = t/t_c$ and $\tilde{u} = u/u_c$, with

$$t_c = \frac{3\mu r_0^2}{\Delta\rho g h_0^3}, \quad u_c = \frac{\Delta\rho g h_0^3}{3\mu r_0}. \tag{2.7a,b}$$

Then, the equation for the horizontal velocity (2.1) and local continuity equation (2.3) can be rewritten in dimensionless form,

$$\tilde{u} = -\tilde{h}^2 \frac{\partial \tilde{h}}{\partial \tilde{r}}, \tag{2.8a}$$

$$\frac{\partial \tilde{h}}{\partial \tilde{t}} + \frac{1}{\tilde{r}} \frac{\partial}{\partial \tilde{r}} (\tilde{r}\tilde{h}\tilde{u}) = -\beta \tilde{h}, \tag{2.8b}$$

where the constant β, which measures the strength of drainage from the permeable boundary, is defined as

$$\beta \equiv \frac{3k_d r_0^2}{d h_0^3}. \tag{2.9}$$

Note that β only involves geometric parameters.

In addition, the governing equation (2.4) for the height of the gravity current h takes the dimensionless form

$$\frac{\partial \tilde{h}}{\partial \tilde{t}} - \frac{1}{\tilde{r}} \frac{\partial}{\partial \tilde{r}} \left(\tilde{r}\tilde{h}^3 \frac{\partial \tilde{h}}{\partial \tilde{r}} \right) = -\beta \tilde{h}. \tag{2.10}$$

The dimensionless initial condition for (2.10) is

$$\tilde{h}(\tilde{r}, 0) = \begin{cases} 1, & 1 \leqslant \tilde{r} < \tilde{r}_{out}, \\ 0, & 0 \leqslant \tilde{r} < 1, \end{cases} \tag{2.11}$$

where $\tilde{r}_{out} \equiv r_{out}/r_0$, and the dimensionless boundary conditions are

$$\frac{\partial \tilde{h}}{\partial \tilde{r}} (\tilde{r}_{out}, \tilde{t}) = 0, \tag{2.12a}$$

$$\tilde{h}(\tilde{r}_f(\tilde{t}), \tilde{t}) = 0, \tag{2.12b}$$

where $\tilde{r}_f(\tilde{t}) \equiv r_f(t)/r_0$. Equation (2.10) together with the boundary and initial conditions (2.11) and (2.12) can be solved numerically to provide the time evolution of the fluid–fluid interface $\tilde{h}(\tilde{r}, \tilde{t})$.

2.3. *Transformation of the problem*

The free-boundary problem of (2.10), subject to (2.11) and (2.12), can be reorganized by introducing new dimensionless variables f and τ based on the following transform (see e.g. Murray 1989; Pritchard *et al.* 2001; Seminara *et al.* 2012):

$$\tilde{h}(\tilde{r}, \tilde{t}) = f(\tilde{r}, \tau) \mathrm{e}^{-\beta \tilde{t}}, \quad \text{where } \tau = \frac{1 - \mathrm{e}^{-3\beta \tilde{t}}}{3\beta}. \tag{2.13a,b}$$

https://doi.org/10.1017/jfm.2015.406 Published online by Cambridge University Press

Note that $\tau \to 0^+$ as $\tilde{t} \to 0^+$, and $\tau \to 1/(3\beta)$ as $\tilde{t} \to +\infty$. Then, (2.10) is transformed to a well-known nonlinear diffusion equation:

$$\frac{\partial f}{\partial \tau} = \frac{1}{\tilde{r}} \frac{\partial}{\partial \tilde{r}} \left(\tilde{r} f^3 \frac{\partial f}{\partial \tilde{r}} \right). \tag{2.14}$$

The initial condition (2.11) can be rewritten as

$$f(\tilde{r}, 0) = \begin{cases} 1, & 1 \leqslant \tilde{r} < \tilde{r}_{out}, \\ 0, & 0 \leqslant \tilde{r} < 1, \end{cases} \tag{2.15}$$

and the boundary conditions (2.12) can be rewritten as

$$\frac{\partial f}{\partial \tilde{r}}(\tilde{r}_{out}, \tau) = 0, \tag{2.16a}$$

$$f(\tilde{r}_f(\tau), \tau) = 0. \tag{2.16b}$$

Thus, the change of variables (2.13) eliminates β from the problem statement and effectively reduces the problem to that of propagation of gravity currents over a rigid impermeable boundary, as has been noted in many of the papers listed in table 1. Now (2.14) can be solved numerically subject to initial condition (2.15) and boundary conditions (2.16) using previously reported algorithms (see e.g. Gratton & Minotti 1990; Diez *et al.* 1992; Zheng *et al.* 2014).

2.4. *Phase-plane analysis*

In order to further study the analytical behaviour of this problem in terms of a second-kind similarity solution, let us now eliminate β from the independent momentum and mass equations (2.8) by introducing a new dimensionless variable v,

$$\tilde{u}(\tilde{r}, \tilde{t}) = v(\tilde{r}, \tau) \mathrm{e}^{-3\beta\tilde{t}}, \tag{2.17}$$

and recall (2.13), so (2.8) can be rewritten as

$$v = -f^2 \frac{\partial f}{\partial \tilde{r}}, \tag{2.18a}$$

$$\frac{\partial f}{\partial \tau} + \frac{1}{\tilde{r}} \frac{\partial}{\partial \tilde{r}} (\tilde{r} f v) = 0. \tag{2.18b}$$

This pair of equations is independent of β and is defined over the time interval $0 \leqslant \tau \leqslant 1/(3\beta)$. We note again that $\tau \to 0^+$ as $\tilde{t} \to 0^+$, and $\tau \to 1/(3\beta)$ as $\tilde{t} \to +\infty$. Now, (2.18) recovers the same governing equations for converging gravity currents on an impermeable horizontal boundary (Gratton & Minotti 1990). For completeness, we give details on conducting a phase-plane analysis based on (2.18), and seek a self-similar solution of the second kind for the time evolution of the fluid–fluid interface.

We assume that there is a finite time t_f, and hence τ_f from (2.13*b*), for the front to reach the origin, and we introduce $s \equiv \tau_f - \tau$, which represents the time remaining for the front to arrive at the origin. We define

$$v(\tilde{r}, \tau) = \frac{\tilde{r}}{s} V(\tilde{r}, s), \quad f(\tilde{r}, \tau) = \left(\frac{\tilde{r}^2}{s} F(\tilde{r}, s) \right)^{1/3}, \tag{2.19a,b}$$

https://doi.org/10.1017/jfm.2015.406 Published online by Cambridge University Press

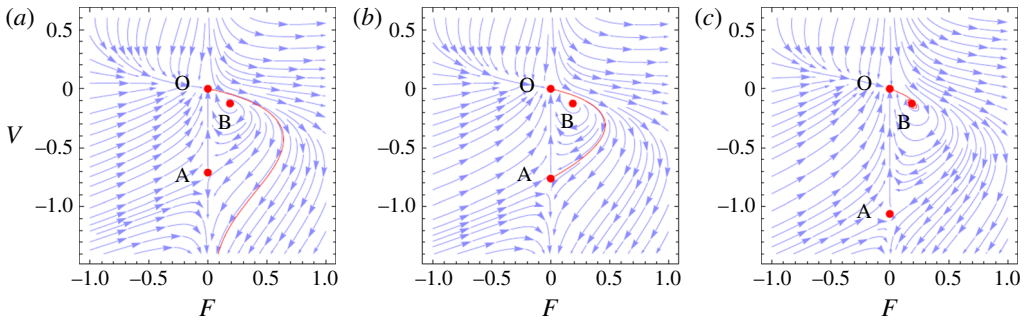

FIGURE 3. (Colour online) The phase plane for the first-order ordinary differential equation (2.22*a*) for different values of δ: (*a*) $\delta = 0.712$, (*b*) $\delta = 0.762$, (*c*) $\delta = 1.06$. In (*b*), the integral curve connects points O and A, thus $\delta = 0.762\ldots$ is the solution to the nonlinear eigenvalue problem.

and substitute (2.19) into (2.18). After some algebra, we obtain the equivalent equations in terms of $V(\tilde{r}, s)$ and $F(\tilde{r}, s)$:

$$3V + \tilde{r}\frac{\partial F}{\partial \tilde{r}} + 2F = 0, \tag{2.20a}$$

$$s\frac{\partial F}{\partial s} - F - 3\tilde{r}F\frac{\partial V}{\partial \tilde{r}} - \tilde{r}V\frac{\partial F}{\partial \tilde{r}} - 8FV = 0. \tag{2.20b}$$

Next, we define the similarity variable $\xi = \tilde{r}/s^{\delta}$, where the scaling exponent δ is to be determined. Then, $F(\tilde{r}, s)$ and $V(\tilde{r}, s)$ become functions of only the similarity variable ξ, i.e. $F = F(\xi)$ and $V = V(\xi)$. In this case, (2.20*a*,*b*) take the self-similar form:

$$3V + \xi F' + 2F = 0, \tag{2.21a}$$

$$\delta\xi F' + F + 3\xi FV' + \xi VF' + 8FV = 0. \tag{2.21b}$$

We can further eliminate ξ in (2.21) and obtain the autonomous forms

$$\frac{\mathrm{d}V}{\mathrm{d}F} = \frac{F(6V - 2\delta + 1) - 3V(V + \delta)}{3F(2F + 3V)}, \tag{2.22a}$$

$$\frac{\mathrm{d}\ln|\xi|}{\mathrm{d}F} = -\frac{1}{2F + 3V}. \tag{2.22b}$$

Equation (2.22*a*) is a first-order nonlinear ordinary differential equation with an unknown parameter δ. Given the value of the parameter δ, the phase portrait of (2.22*a*) can be obtained; different solution curves in the phase portrait represent different self-similar flows subject to different boundary conditions, see figure 3.

The boundary conditions of a specific physical problem are associated with the critical points in (2.22*a*) in the phase plane (see e.g. Gratton & Minotti 1990). By letting the numerator and denominator be equal to zero, we obtain three finite critical points in the phase plane of (2.22*a*):

$$\text{O: } (F, V) = (0, 0), \tag{2.23a}$$

$$\text{A: } (F, V) = (0, -\delta), \tag{2.23b}$$

$$\text{B: } (F, V) = \left(\tfrac{3}{16}, -\tfrac{1}{8}\right). \tag{2.23c}$$

https://doi.org/10.1017/jfm.2015.406 Published online by Cambridge University Press

Experiment	Permeability k_d (10^{-8} m^2)	Thickness d (10^{-3} m)	Initial height h_0 (m)	'Touch-down' time t_f (s)	Parameter β
1	0	—	0.020	12.5	0
2	0	—	0.030	5.01	0
3	3.9	3.2	0.029	19.4	0.019
4	3.9	3.2	0.030	16.1	0.017
5	3.9	3.2	0.031	13.1	0.015
6	3.9	3.2	0.033	8.55	0.012
7	5.0	6.4	0.029	11.1	0.012
8	13	1.6	0.043	6.34	0.017
9	13	1.6	0.046	5.14	0.014
10	13	1.6	0.055	2.47	0.0082
11	3.9	3.2	0.013	$+\infty$	0.207
12	3.9	3.2	0.020	$+\infty$	0.057

TABLE 2. Summary of experiments on viscous converging gravity currents spreading over impermeable and permeable horizontal substrates. In all of the experiments golden syrup was used as the viscous fluid, and the viscosity μ and density ρ were measured: $\mu = 7.6$ Pa s and $\rho = 1.47 \times 10^3$ kg m^{-3}. The outer radius of the cylindrical tank is $r_{out} = 0.147$ m, and the location of the lock gate is $r_0 = 0.112$ m. The 'touch-down' time t_f is defined as the time for the front to arrive at the centre of the tank. The dimensionless parameter β is calculated based on (2.9).

Point A describes a state of zero height and finite velocity, which corresponds to the moving front of the gravity current, where $h(r_f(t), t) = 0$ and $\mathrm{d}r_f(t)/\mathrm{d}t \neq 0$. Point O corresponds to the state when $s = 0$, i.e. $\tau = \tau_f$ (see e.g. Gratton & Minotti 1990). Physically, point O corresponds to the state when the front arrives at the origin, i.e. the centre of the cylinder. Thus, the integral curve connecting points O and A in the phase plane describes an inwardly converging viscous gravity current when the front is near the origin.

In order to obtain the integral curve connecting points O and A, we first linearize (2.22*a*) near point O, and we obtain the eigenspace:

$$\lambda_1 = -3\delta, \quad \boldsymbol{e}_1 = (0, \pm 1), \tag{2.24a}$$

$$\lambda_2 = 0, \quad \boldsymbol{e}_2 = \pm\left(\frac{3\delta}{1-2\delta}, 1\right). \tag{2.24b}$$

To solve (2.22*a*) subject to (2.23*a*,*b*), we start from an initial condition (F_i, V_i) slightly perturbed from point O in the neutral eigendirection given by $\boldsymbol{e}_2$. Given a value of δ, the integral curve starting from (F_i, V_i) can be calculated numerically using the built-in Mathematica subroutine NDSolve, as shown in figure 3. Then, we adjust the values of δ, and we observe that the integral curve connects to point A only when $\delta = 0.762\ldots$, see figure 3, which agrees with the calculation of Gratton & Minotti (1990). Thus, we have found a second-kind self-similar solution for the converging gravity currents with vertical fluid leakage through a permeable substrate.

3. Experimental observations

We have conducted a series of experiments on a viscous converging gravity current using Lyle's golden syrup, see table 2. The viscosity and density were measured,

https://doi.org/10.1017/jfm.2015.406 Published online by Cambridge University Press

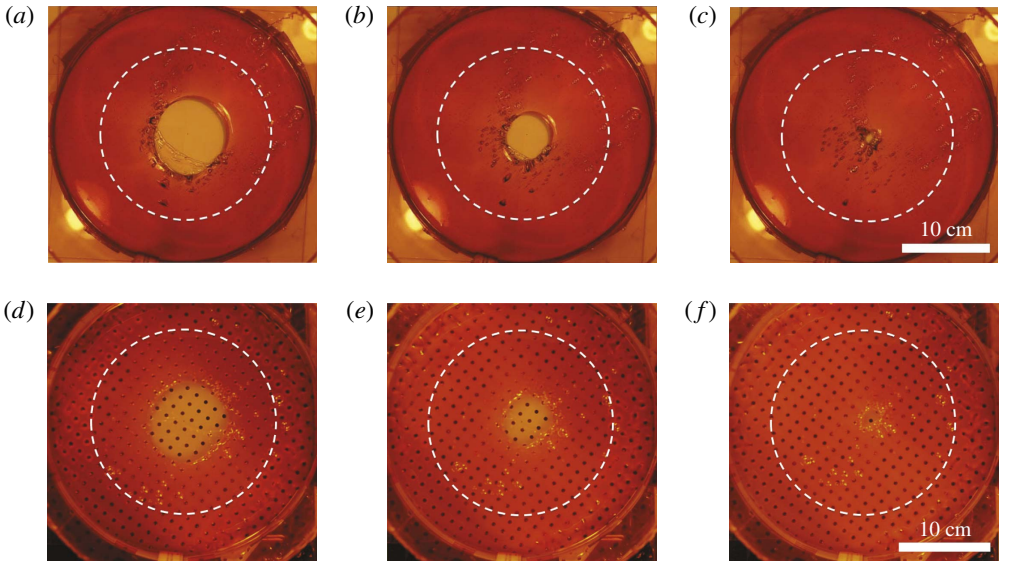

FIGURE 4. (Colour online) Typical experimental observations of viscous converging gravity currents: (*a–c*) over an impermeable substrate, experiment 2 in table 2; (*d–f*) over a thin perforated plate with vertical fluid drainage, experiment 4 in table 2. The dashed circle indicates the location of the cylindrical lock gate at the beginning of the experiments. Golden syrup was used as the viscous fluid in the experiments. Time from start of experiment: (*a*) 1.67 s; (*b*) 2.94 s; (*c*) 4.71 s; (*d*) 4.34 s; (*e*) 8.09 s; (*f*) 15.10 s.

respectively, to be $\mu = 7.6$ Pa s and $\rho = 1.47 \times 10^3$ kg m^{-3}. In the experiments, a cylindrical lock gate of radius $r_0 = 0.112$ m was used to create the horizontal inward flow within a cylindrical tank of radius $r_{out} = 0.147$ m. Several perforated plates (with different permeability due to changing distributions of holes) were used as the bottom leaky boundary such that slow fluid drainage occurs during the spreading of the current. A digital camera was installed above the experimental set-up to capture from the top the time evolution of the gravity currents. Typical experimental pictures are shown in figure 4.

3.1. *Permeability estimates*

In estimating the permeability k_d (see (2.2)) of the perforated plates in our experiments, we use

$$k_d = \phi k_{hole}, \tag{3.1}$$

where ϕ denotes the porosity of the substrate and k_{hole} is the permeability of each hole (see e.g. Bear 1972; Phillips 1991). The well-known result from the Poiseuille model gives

$$k_{hole} = r_{hole}^2/8, \tag{3.2}$$

where r_{hole} represents the radius of the parallel circular holes. When the holes are short, the resistance to flow entering and exiting the holes also needs to be considered besides the wall friction along the hole; for example, see (5) in Jensen *et al.* (2014), and for more discussions see e.g. Sampson (1891), Weissberg (1962) and Dagan *et al.* (1982). The interactions of flows entering and exiting each hole may also need to be considered when the spaces between the holes are small; a correction coefficient G is

https://doi.org/10.1017/jfm.2015.406 Published online by Cambridge University Press

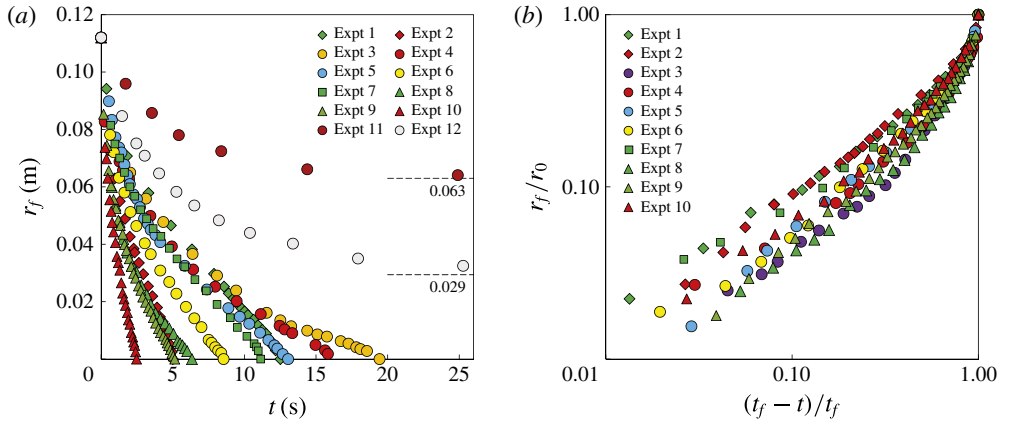

FIGURE 5. (Colour online) Time evolution of the front locations from our experiments on viscous converging gravity currents with fluid drainage through the permeable substrate. In (*a*), the location of the lock gate is 0.112 m, which provides the initial value for all experiments. In (*b*), r_0 is the location of the lock gate; t_f represents the time for the front to arrive at the centre of the tank, which can be read in (*a*) as the intercept with the horizontal axis (except for experiments 11 and 12, which stop at a stationary non-zero radial position).

provided for both square and hexagonal arrays, see (16) and figure 5 in Jensen *et al.* (2014). In our data analysis, in estimating k_{hole} for each hole, we combined (5) and (16) in Jensen *et al.* (2014), and we obtain:

$$k_{hole} = \left(\frac{8}{r_{hole}^2} + \frac{3\pi(1-G)}{r_{hole} d} \right)^{-1}, \tag{3.3}$$

where d is thickness of the plate and G is the correction coefficient. For example, one perforated plate in our experiments contains parallel circular holes of radius $r_{hole} \approx 1.6$ mm in hexagonal arrays, and the centre-to-centre distance between each pair of holes is $L \approx 2.6$ mm. The thickness of the plate is $d \approx 1.6$ mm. With $G \approx 0.13$ from figure 5 of Jensen *et al.* (2014), then based on (3.3), the permeability of each hole is $k_{hole} \approx 1.6 \times 10^{-7}$ m^2. The porosity of the plate is $\phi \approx 0.42$, and hence the permeability is $k_d \approx 6.6 \times 10^{-8}$ m^2. As a comparison, based on the Poiseuille model (3.2) alone, $k_{hole} \approx 3.2 \times 10^{-7}$ m^2 and $k_d \approx 1.3 \times 10^{-7}$ m^2. As can be seen, both k_{hole} and k_d are smaller than the estimates from the Poiseuille model, because of the second term in the denominator of (3.3), which indicates the effect of resistance to flow entering and exiting the holes.

3.2. *Front propagation law*

We track the locations of the moving front as a function of time, as shown in figure 5. Then, we plot the time evolution of the front locations in the rescaled coordinates, i.e. r_f/r_0 versus $(\tau_f - \tau)/\tau_f$, see figure 6. Note that the front is not perfectly circular during the propagation process, so we have used an effective radius r_{eff} in our data analysis, defined as $r_{eff} \equiv (A/\pi)^{1/2}$, where A denotes the area formed by the moving front. Numerical solutions of the PDE (2.14) subject to initial condition (2.15) and boundary conditions (2.16) are also plotted. The dashed line in figure 6 indicates the slope of 0.762, which comes from the prediction of the second-kind self-similar

https://doi.org/10.1017/jfm.2015.406 Published online by Cambridge University Press

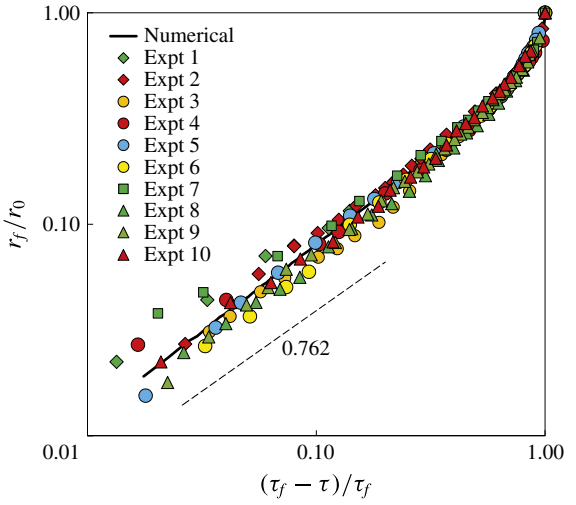

FIGURE 6. (Colour online) Experimental results of the front locations versus the prediction of numerical simulations (axes are log–log). The theoretical slope of 0.762 is shown, which is the prediction of the second-kind self-similar solution. We only show the numerical results for experiment 3 since the calculations only show slight differences for experiments 1–10 in table 2 in this plot (the differences are due to different initial conditions). τ_f is defined based on (2.13*b*).

solution (§ 2.4). Good agreement is observed among the experimental, numerical and theoretical results.

3.3. *Will the front reach the origin?*

When the initial height is very small in the experiments, e.g. experiments 11 and 12 in table 2, we have observed that the front stops and does not reach the centre of the tank. This result is different from the prediction of the gravity current model without drainage. Note that the height of the gravity current decreases during the experiments because of horizontal spreading and vertical drainage through the permeable substrate; and the vertical drainage prevents the converging front from reaching the centre of the tank for a small initial height.

A numerical simulation has been conducted by solving (2.14) subject to initial condition (2.15) and boundary conditions (2.16). The simulation stops at $\tau = 1/(3\beta)$, which corresponds to $\tilde{t} \to +\infty$. The final location of the front, defined as

$$r_\infty \equiv \lim_{\tilde{t}\to+\infty} r_f(\tilde{t}), \tag{3.4}$$

can be obtained through the numerical simulations. To demonstrate the idea, we have chosen $r_{out}/r_0 \approx 1.31$ (based on our experiments), and we show, in figure 7, the relationship between the final front location r_∞/r_0 and the drainage constant β. When $\beta \geqslant \beta_c \approx 0.058$, the drainage effect becomes important, and the front does not reach the origin. As β continues to increase, the effect of drainage becomes more important, and the final front location increases. Experimental measurements of the final front locations have also been plotted in figure 7, and we have observed good agreement. The error bar indicates a 10 % error for the value of the dimensionless parameters

https://doi.org/10.1017/jfm.2015.406 Published online by Cambridge University Press

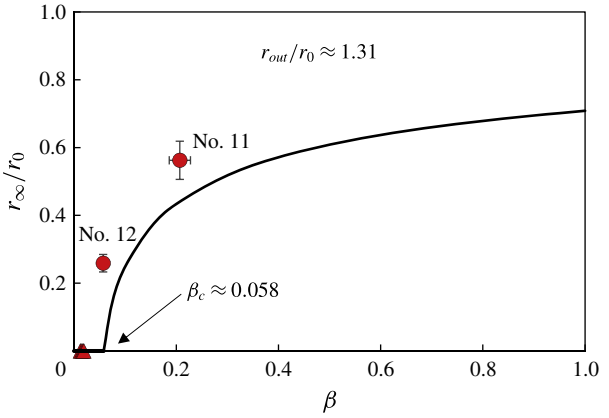

FIGURE 7. (Colour online) The final location of the propagating front r_∞/r_0 depends on the value of drainage constant β, defined in (2.9), which only involves geometric parameters. We have set $r_{out}/r_0 \approx 1.31$ in the numerical calculation, based on our experiments. When $\beta > \beta_c \approx 0.058$, the front does not reach the origin. The observations from experiments 3–6 and 11–12 are also shown in this figure. The error bar represents a 10 % error in the estimates for the final front location r_∞/r_0 and the drainage constant β.

r_∞/r_0 and β. Note that the theoretical predictions are smaller than the experimental observations. This is likely due to the effect of surface tension and contact angle in our experiments when the height of the gravity current is small at late times. We note that the capillary length scale in a typical experiment is $l_c \equiv \sqrt{\gamma/(\Delta\rho g)} \approx 2.4$ mm, where we use $\gamma \approx 80$ mN m^{-1} for golden syrup. Thus, when the film thickness approaches this length scale at late times, capillary effects become more important.

In addition, depending on the values of the two dimensionless parameters r_0/r_{out} and β, a regime plot can be obtained that describes whether the front reaches the origin or not (figure 8): a 'touching' regime in which the front reaches the origin, and a 'non-touching' regime in which the front does not arrive at the origin. For a given r_{out}/r_0, the front does not reach the origin when the drainage constant β becomes greater than a critical value β_c, which is calculated numerically in this figure (the black curve). Information from our experiments has also been plotted in the regime diagram.

There are other effects that can contribute to the uncertainty of the experiments besides the effect of surface tension and contact angle. For example, we have neglected the effect of leakage through the gap between the substrate and the bottom of the lock gate at the beginning of the experiments; we also neglected the amount of fluid that attaches to the lock gate and hence leaves the system when we remove the lock gate. The error in the measurements of the initial height, the density and viscosity of golden syrup can also contribute to the uncertainty of our experiments. Overall the errors are relatively small and we obtain good agreement with the numerical and theoretical predictions.

4. Generalizations and discussions

In this section, we generalize our discussion and analysis to two more categories of gravity current spreading problems where vertical fluid drainage occurs through the permeable horizontal substrate. In particular, we consider the flow situations where second-kind self-similar solutions are available for the analogous 'converging'

https://doi.org/10.1017/jfm.2015.406 Published online by Cambridge University Press

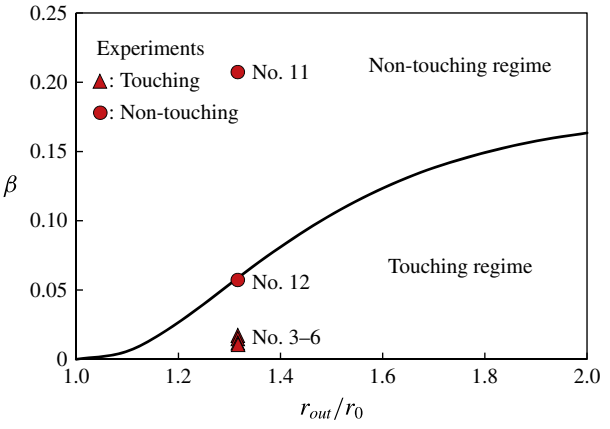

FIGURE 8. (Colour online) Regime diagram that describes whether the front reaches the origin (i.e. 'touching' regime) or not (i.e. 'non-touching' regime). For a given r_{out}/r_0, the front does not reach the origin when the drainage constant β is greater than a critical value β_c, calculated numerically in this plot (the black curve). The observations from experiments 3–6 and 11–12 are also shown in this diagram.

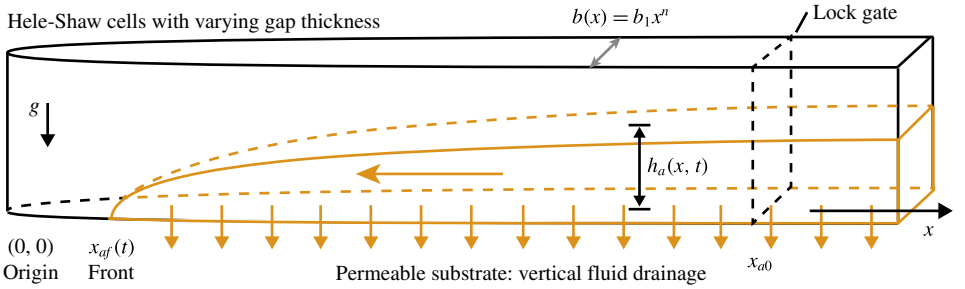

FIGURE 9. (Colour online) Propagation of a viscous gravity current towards the origin in a Hele-Shaw cell with varying gap thickness $b(x)$ in the horizontal direction. The substrate is permeable such that fluid drainage occurs in the vertical direction.

flow problems without vertical fluid drainage: (i) the propagation of viscous gravity currents in Hele-Shaw channels with varying gap thickness (figure 9); and (ii) the propagation of gravity currents in porous media with horizontal permeability and porosity gradients (figure 12). We introduce appropriate mathematical transforms on time, horizontal velocity and the height of the current so that the theoretical models of spreading with boundary seepage can be mapped to the analogous models describing the flow situations without vertical fluid drainage (Zheng *et al.* 2014). A summary of the theoretical models is provided in table 3. Our work can provide insights into real flow situations in a crack or in a porous medium with horizontal heterogeneities and permeable boundaries (see e.g. Bear 1972; Phillips 1991; Class & Ebigbo 2009).

4.1. *Hele-Shaw channels with varying gap thickness*

We consider viscous gravity currents spreading in Hele-Shaw cells with varying gap thickness $b(x) = b_1 x^n$ in the horizontal direction (figure 9). In our previous work, we found a second-kind self-similar solution for $0 < n < 1$, when the gravity current

https://doi.org/10.1017/jfm.2015.406 Published online by Cambridge University Press

https://doi.org/10.1017/jfm.2015.406 Published online by Cambridge University Press

	Cylindrical tanks	Hele-Shaw cells	Porous media
Horizontal velocity	$\tilde{u} = -\tilde{h}^2 \dfrac{\partial \tilde{h}}{\partial \tilde{r}}$	$\tilde{u}_a = -\tilde{x}^{2n} \dfrac{\partial \tilde{h}_a}{\partial \tilde{x}}$	$\tilde{u}_p = -\tilde{x}^{n} \dfrac{\partial \tilde{h}_p}{\partial \tilde{x}}$
Continuity equation	$\dfrac{\partial \tilde{h}}{\partial \tilde{t}} + \dfrac{1}{\tilde{r}} \dfrac{\partial}{\partial \tilde{r}} (\tilde{r}\tilde{h}\tilde{u}) = -\beta \tilde{h}$	$\dfrac{\partial \tilde{h}_a}{\partial \tilde{t}} + \dfrac{1}{\tilde{x}^n} \dfrac{\partial}{\partial \tilde{x}} (\tilde{x}^n \tilde{h}_a \tilde{u}_a) = -\beta_a \tilde{h}_a$	$\dfrac{\partial \tilde{h}_p}{\partial \tilde{t}} + \dfrac{1}{\tilde{x}^m} \dfrac{\partial}{\partial \tilde{x}} (\tilde{h}_p \tilde{u}_p) = -\beta_p \tilde{h}_p$
Interface shape	$\dfrac{\partial \tilde{h}}{\partial \tilde{t}} - \dfrac{1}{\tilde{r}} \dfrac{\partial}{\partial \tilde{r}} \left(\tilde{r}\tilde{h}^3 \dfrac{\partial \tilde{h}}{\partial \tilde{r}} \right) = -\beta \tilde{h}$	$\dfrac{\partial \tilde{h}_a}{\partial \tilde{t}} - \dfrac{1}{\tilde{x}^n} \dfrac{\partial}{\partial \tilde{x}} \left(\tilde{x}^{3n} \tilde{h}_a \dfrac{\partial \tilde{h}_a}{\partial \tilde{x}} \right) = -\beta_a \tilde{h}_a$	$\dfrac{\partial \tilde{h}_p}{\partial \tilde{t}} - \dfrac{1}{\tilde{x}^m} \dfrac{\partial}{\partial \tilde{x}} \left(\tilde{x}^{n} \tilde{h}_p \dfrac{\partial \tilde{h}_p}{\partial \tilde{x}} \right) = -\beta_p \tilde{h}_p$
Drainage constant	$\beta \equiv \dfrac{3k_d r_0^2}{dh_0^3}$	$\beta_a \equiv \dfrac{12k_d x_{a0}^{2-2n}}{dh_{a0} b_1^2}$	$\beta_p \equiv \dfrac{k_d}{x_{p0}^{n-m} k_1 \, dh_{p0}}$
Mathematical transforms	$\tilde{h}(\tilde{r}, \tilde{t}) = f(\tilde{r}, \tau) \mathrm{e}^{-\beta \tilde{t}}$	$\tilde{h}_a(\tilde{r}, \tilde{t}) = f_a(\tilde{r}, \tau) \mathrm{e}^{-\beta_a \tilde{t}}$	$\tilde{h}_p(\tilde{r}, \tilde{t}) = f_p(\tilde{r}, \tau) \mathrm{e}^{-\beta_p \tilde{t}}$
	$\tilde{u}(\tilde{r}, \tilde{t}) = v(\tilde{r}, \tau) \mathrm{e}^{-3\beta \tilde{t}}$	$\tilde{u}_a(\tilde{r}, \tilde{t}) = v_a(\tilde{r}, \tau) \mathrm{e}^{-\beta_a \tilde{t}}$	$\tilde{u}_p(\tilde{r}, \tilde{t}) = v_p(\tilde{r}, \tau) \mathrm{e}^{-\beta_p \tilde{t}}$
	$\tau = \dfrac{1 - \mathrm{e}^{-3\beta \tilde{t}}}{3\beta}$	$\tau = \dfrac{1 - \mathrm{e}^{-\beta_a \tilde{t}}}{\beta_a}$	$\tau = \dfrac{1 - \mathrm{e}^{-\beta_p \tilde{t}}}{\beta_p}$
As $\tilde{t} \to +\infty$	$\tau \to 1/(3\beta)$	$\tau \to 1/\beta_a$	$\tau \to 1/\beta_p$
After transform:			
Horizontal velocity	$v = -f^2 \dfrac{\partial f}{\partial \tilde{r}}$	$v_a = -\tilde{x}^{2n} \dfrac{\partial f_a}{\partial \tilde{x}}$	$v_p = -\tilde{x}^{n} \dfrac{\partial f_p}{\partial \tilde{x}}$
Continuity equation	$\dfrac{\partial f}{\partial \tau} + \dfrac{1}{\tilde{r}} \dfrac{\partial}{\partial \tilde{r}} (\tilde{r} f v) = 0$	$\dfrac{\partial f_a}{\partial \tau} + \dfrac{1}{\tilde{x}^n} \dfrac{\partial}{\partial \tilde{x}} (\tilde{x}^n f_a v_a) = 0$	$\dfrac{\partial f_p}{\partial \tau} + \dfrac{1}{\tilde{x}^m} \dfrac{\partial}{\partial \tilde{x}} (f_p v_p) = 0$
Interface shape	$\dfrac{\partial f}{\partial \tau} = \dfrac{1}{\tilde{r}} \dfrac{\partial}{\partial \tilde{r}} \left(\tilde{r} f^3 \dfrac{\partial f}{\partial \tilde{r}} \right)$	$\dfrac{\partial f_a}{\partial \tau} = \dfrac{1}{\tilde{x}^n} \dfrac{\partial}{\partial \tilde{x}} \left(\tilde{x}^{3n} f_a \dfrac{\partial f_a}{\partial \tilde{x}} \right)$	$\dfrac{\partial f_p}{\partial \tau} = \dfrac{1}{\tilde{x}^m} \dfrac{\partial}{\partial \tilde{x}} \left(\tilde{x}^{n} f_p \dfrac{\partial f_p}{\partial \tilde{x}} \right)$

TABLE 3. Theoretical models on the propagation of viscous gravity currents on thin permeable horizontal substrates with vertical fluid drainage through the substrates. n and m indicate the horizontal heterogeneities, as defined in § 4.

propagates towards the origin, where the gap thickness is zero (Zheng *et al.* 2014). Now, let us consider the same problem but with vertical fluid drainage from a thin permeable bottom boundary of permeability k_d and thickness d. The origin of the coordinate system is defined as the location of zero gap thickness, i.e. $b(0) = 0$. The height of the gravity current and the horizontal velocity are denoted by $h_a(x, t)$ and $u_a(x, t)$, and initially fluid of height h_{a0} is confined by a lock gate at location x_{a0}. Assuming $d \ll h_a$ for the majority part of the current away from the moving front, using Darcy's law and the local continuity equation, we obtain

$$u_a = -\frac{\Delta\rho g b_1^2}{12\mu} x^{2n} \frac{\partial h_a}{\partial x}, \tag{4.1a}$$

$$\frac{\partial h_a}{\partial t} + \frac{1}{x^n}\frac{\partial}{\partial x}(x^n h_a u_a) = -\frac{\Delta\rho g k_d h_a}{\mu d}. \tag{4.1b}$$

Let us now define dimensionless variables $\tilde{h}_a \equiv h_a/h_{a0}$, $\tilde{u}_a \equiv 12\mu u_a/(\Delta\rho g b_1^2 x_{a0}^{2n-1} h_{a0})$, $\tilde{x} \equiv x/x_{a0}$, and $\tilde{t} \equiv \Delta\rho g b_1^2 x_{a0}^{2n-2} h_{a0} t/(12\mu)$. Then, the dimensionless forms of the governing equations (4.1) become

$$\tilde{u}_a = -\tilde{x}^{2n} \frac{\partial \tilde{h}_a}{\partial \tilde{x}}, \tag{4.2a}$$

$$\frac{\partial \tilde{h}_a}{\partial \tilde{t}} + \frac{1}{\tilde{x}^n}\frac{\partial}{\partial \tilde{x}}(\tilde{x}^n \tilde{h}_a \tilde{u}_a) = -\beta_a \tilde{h}_a, \tag{4.2b}$$

where the dimensionless parameter β_a measures the significance of vertical fluid drainage from the permeable horizontal boundary, and is defined as

$$\beta_a \equiv \frac{12 k_d x_{a0}^{2-2n}}{d h_{a0} b_1^2}. \tag{4.3}$$

Now we introduce the following transform:

$$\tilde{h}_a(\tilde{r}, \tilde{t}) = f_a(\tilde{r}, \tau)\mathrm{e}^{-\beta_a \tilde{t}}, \quad \tilde{u}_a(\tilde{r}, \tilde{t}) = v_a(\tilde{r}, \tau)\mathrm{e}^{-\beta_a \tilde{t}}, \quad \tau = \frac{1 - \mathrm{e}^{-\beta_a \tilde{t}}}{\beta_a}. \tag{4.4a–c}$$

Immediately, we note that $\tau \to 0^+$ as $\tilde{t} \to 0^+$, and $\tau \to 1/\beta_a$ as $\tilde{t} \to +\infty$. In addition, (4.2) are transformed to

$$v_a = -\tilde{x}^{2n} \frac{\partial f_a}{\partial \tilde{x}}, \tag{4.5a}$$

$$\frac{\partial f_a}{\partial \tau} + \frac{1}{\tilde{x}^n}\frac{\partial}{\partial \tilde{x}}(\tilde{x}^n f_a v_a) = 0. \tag{4.5b}$$

Note that (4.5) has the same form as (2.10) in Zheng *et al.* (2014), which describes the propagation of viscous gravity currents in a Hele-Shaw cell with an impermeable substrate. Then, a second-kind self-similar solution can be derived following § 2.1.2 of Zheng *et al.* (2014), when the current propagates towards the origin:

$$v_a(\tilde{x}, \tau) = \frac{\tilde{x}}{s} V_a(\xi), \quad f_a(\tilde{x}, \tau) = \frac{\tilde{x}^{2(1-n)}}{s} F_a(\xi), \tag{4.6a,b}$$

where $s \equiv \tau_f - \tau$, indicating the time remaining for the front to reach the origin, and the similarity variable is defined as $\xi \equiv \tilde{x}/s^\delta$. The scaling exponent $\delta(n)$ depends on n,

https://doi.org/10.1017/jfm.2015.406 Published online by Cambridge University Press

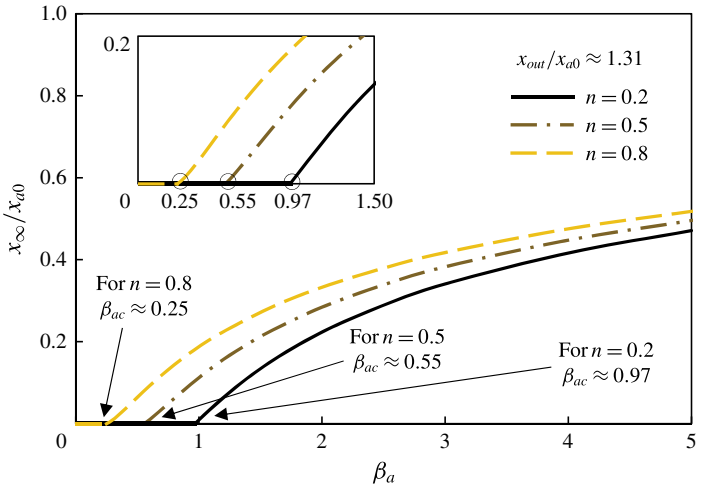

FIGURE 10. (Colour online) The final location of the propagating front x_∞/x_{a0} depends on the value of drainage constant β_a, defined in (4.3), and the geometric parameter n for the shape of the channel. We have set $x_{out}/x_{a0} \approx 1.31$ in the numerical calculation, to be consistent with § 3. When $\beta > \beta_{ac}(n)$, the front does not reach the origin; the value of $\beta_{ac}(n)$ depends on n, and we have shown the numerical calculations for $n = 0.2, 0.5, 0.8$ in this figure.

and can be obtained (for $0 < n < 1$) by solving a nonlinear eigenvalue problem using a phase-plane analysis, for example, $\delta(0.2) \approx 1.14$, $\delta(0.5) \approx 1.54$ and $\delta(0.8) \approx 2.95$ from figure 6 of Zheng *et al.* (2014).

It should also be noted that when the drainage effect becomes important, the front will not be able to reach the origin. We show the final location of the propagating front x_∞, defined as $x_\infty \equiv \lim_{\tilde{t}\to+\infty} x(\tilde{t})$, for $x_{out}/x_{a0} \approx 1.31$ in figure 10, based on a numerical calculation. Note that x_{out} represents the horizontal span of the channel, and x_{a0} is the location of the lock gate. When the drainage constant β_a, defined in (4.3), becomes greater than a critical value $\beta_{ac}(n)$ (which depends on n, the shape parameter of the channel), the front does not reach the origin. A regime diagram (figure 11) can also be obtained for different values of the drainage constant β_a, the dimensionless parameter x_{out}/x_{a0} and the shape parameter n for the channel. Analogously to the discussion in § 3.3, a 'touching' regime and a 'non-touching' regime can be identified.

4.2. *Porous media with horizontal permeability and porosity gradients*

Let us now study the propagation of a viscous gravity current in porous media with permeability and porosity gradients of power-law forms in the horizontal direction: $k(x) = k_1 x^n$ and $\phi(x) = \phi_1 x^m$ (figure 12). We note that, in practice, $2 < n/m < 3$, where $n/m = 2$ represents a porous medium of tubular holes, and $n/m = 3$ represents a network of intersecting fissures, as mentioned in Phillips (1991). We allow slow fluid drainage from the thin permeable substrate of permeability k_d and thickness d. The origin of the coordinate system is placed at the location of zero permeability and porosity, i.e. $k(0) = 0$ and $\phi(0) = 0$. We denote the height of the current and the horizontal velocity as $h_p(x, t)$ and $u_p(x, t)$, and we assume that initially the fluid of height h_{p0} is confined by a lock gate at x_{p0}. Then, analogously to the development in

https://doi.org/10.1017/jfm.2015.406 Published online by Cambridge University Press

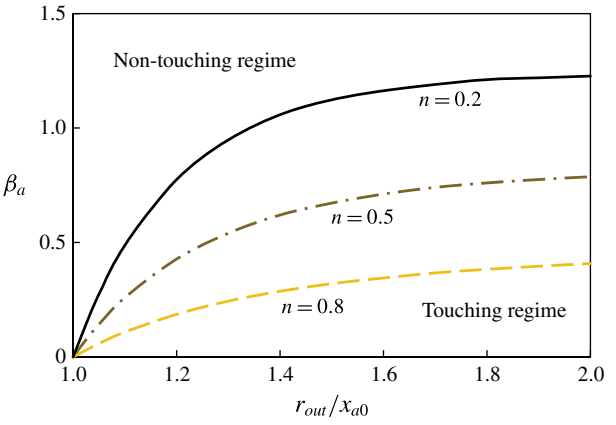

FIGURE 11. (Colour online) Regime diagram that describes whether the front reaches the origin (i.e. 'touching' regime) or not (i.e. 'non-touching' regime). For a given x_{out}/x_{a0}, the front does not reach the origin when the drainage constant β_a is greater than a critical value $\beta_{ac}(n)$ (shown as the curves for $n = 0.2, 0.5, 0.8$), which also depends on the geometric parameter n for the shape of the channel.

§ 4.1, the governing equations for the fluid flow are written as

$$u_p = -\frac{\Delta\rho g k_1 x^n}{\mu}\frac{\partial h_p}{\partial x}, \tag{4.7a}$$

$$\frac{\partial h_p}{\partial t} + \frac{1}{\phi_1 x^m}\frac{\partial}{\partial x}(h_p u_p) = -\frac{\Delta\rho g k_d h}{\phi_1 \mu d}. \tag{4.7b}$$

Again, we non-dimensionalize (4.7) by defining dimensionless variables $\tilde{h}_p \equiv h_p/h_{p0}$, $\tilde{u}_p \equiv \mu u_p/(\Delta\rho g k_1 x_{p0}^{n-1} h_{p0})$, $\tilde{x} \equiv x/x_{p0}$ and $\tilde{t} \equiv \Delta\rho g k_1 x_{p0}^{n-m} h_{p0} t/(\phi_1 \mu)$. Then, the dimensionless form of governing equation (4.7) becomes

$$\tilde{u}_p = -\tilde{x}^n \frac{\partial \tilde{h}_p}{\partial \tilde{x}}, \tag{4.8a}$$

$$\frac{\partial \tilde{h}_p}{\partial \tilde{t}} + \frac{1}{\tilde{x}^m}\frac{\partial}{\partial \tilde{x}}(\tilde{h}_p \tilde{u}_p) = -\beta_p \tilde{h}_p, \tag{4.8b}$$

where a dimensionless parameter β_p is defined as

$$\beta_p \equiv \frac{k_d}{x_{p0}^{n-m} k_1\, d h_{p0}}, \tag{4.9}$$

which measures the significance of the vertical fluid drainage. Then, we can introduce the following transform:

$$\tilde{h}_p(\tilde{r}, \tilde{t}) = f_p(\tilde{r}, \tau)\mathrm{e}^{-\beta_p \tilde{t}}, \quad \tilde{u}_p(\tilde{r}, \tilde{t}) = v_p(\tilde{r}, \tau)\mathrm{e}^{-\beta_p \tilde{t}}, \quad \tau = \frac{1 - \mathrm{e}^{-\beta_p \tilde{t}}}{\beta_p}, \tag{4.10a–c}$$

and we note that $\tau \to 0^+$ as $\tilde{t} \to 0^+$, and $\tau \to 1/\beta_p$ as $\tilde{t} \to +\infty$. We can also transform equation (4.8) into

$$v_p = -\tilde{x}^n \frac{\partial f_p}{\partial \tilde{x}}, \tag{4.11a}$$

https://doi.org/10.1017/jfm.2015.406 Published online by Cambridge University Press

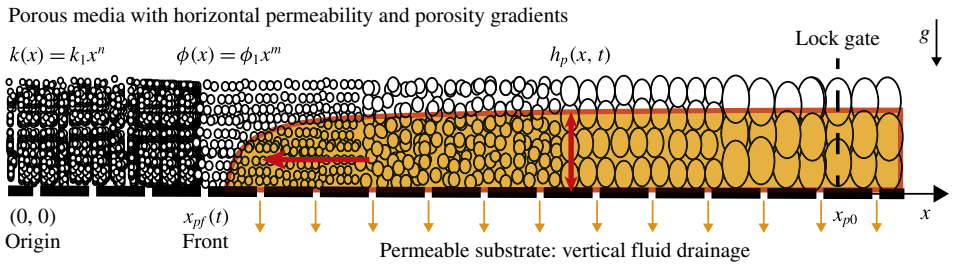

FIGURE 12. (Colour online) Propagation of a viscous gravity current towards the origin in a porous medium with horizontal permeability and porosity gradients. The substrate is permeable such that fluid drainage occurs in the vertical direction.

$$\frac{\partial f_p}{\partial \tau} + \frac{1}{\tilde{x}^m}\frac{\partial}{\partial \tilde{x}}(f_p v_p) = 0. \tag{4.11b}$$

Again, we observe that (4.11) has the same form as (2.27) in Zheng *et al.* (2014), which describes the propagation of a gravity current on an impermeable substrate. Therefore, a second-kind self-similar solution can be obtained following § 2.2.2 of Zheng *et al.* (2014). Let us denote $s = \tau_f - \tau$, representing the remaining time for the front to arrive at the origin; then, the self-similar solution is given by

$$v_p(\tilde{x}, \tau) = \frac{\tilde{x}^{m+1}}{s} V_p(\xi), \quad f_p(\tilde{x}, \tau) = \frac{\tilde{x}^{m-n+2}}{s} F_p(\xi), \tag{4.12a,b}$$

where the similarity variable ξ is defined as $\xi \equiv \tilde{x}/s^{\delta}$, and the scaling exponent $\delta(m, n)$, depending on both m and n, can be obtained by solving a nonlinear eigenvalue problem, for example, $\delta(1, 2.5) \approx 2.42$ and $\delta(1.5, 3.1) \approx 2.78$.

We also note that as the drainage constant β_p increases, the effect of fluid loss through drainage becomes more significant, and eventually the front may not reach the origin. Similar to the analysis in §§ 3.3 and 4.1, we are able to numerically calculate the final location of the propagating front x_∞, defined as $x_\infty \equiv \lim_{\tilde{t}\to+\infty} x(\tilde{t})$, and we show the results in figure 13(*a*). We have chosen ($m = 1$, $n = 2.5$) and ($m = 1.5$, $n = 3.1$) in the numerical calculations as examples; we have also chosen $x_{out}/x_{p0} \approx 1.31$ to be consistent with the analysis in §§ 3.3 and 4.1. In addition, we obtain a regime diagram (figure 13*b*) that characterizes whether or not the front reaches the origin, depending on the drainage constant β_p, the dimensionless parameter x_{out}/x_{p0} and the values of m and n that describe the horizontal heterogeneity of the porous medium. Note that x_{out} represents the horizontal span of the porous medium and x_{p0} denotes the location of the lock gate.

5. Final remarks

It is well known that the spreading of gravity currents can be described by similarity solutions of the first kind so that dimensional reasoning, along with the structure of the PDE, yields the shape and spreading characteristics. It is well appreciated that, for simple models of leakage through a substrate, analysis of the spreading problem is still possible via a change of variables (2.13) that reduces the problem to one previously studied. Many problems of this type have been reported (see table 1).

As first summarized for gravity currents without leakage by Gratton & Minotti (1990), a self-similar solution of the second kind can also be obtained to describe the

https://doi.org/10.1017/jfm.2015.406 Published online by Cambridge University Press

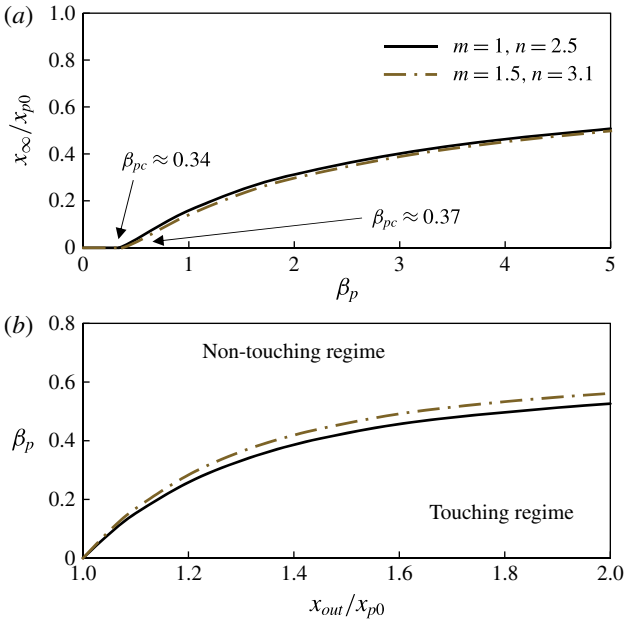

FIGURE 13. In (*a*), the final location x_∞ of the front depends on the drainage constant β_p, and the values of m and n that describe the horizontal heterogeneity of the porous medium. We have chosen ($m = 1$, $n = 2.5$) and ($m = 1.5$, $n = 3.1$) as examples; we have also chosen $x_{out}/x_{p0} \approx 1.31$ to be consistent with §§ 4.1 and 3.3. In (*b*), the regime diagram is shown and describes whether or not the front arrives at the origin in a porous medium with horizontal permeability and porosity gradients.

interface shape when the currents propagate towards an 'origin'. Here we report the effect of fluid drainage on second-kind self-similar solutions for the time evolution of the fluid–fluid interface. By extending the change of variables (2.13) to include velocity (2.17), we map the original problem to the analogous flow situations without vertical fluid drainage (summarized in table 3); then, various self-similar solutions of the second kind can be obtained by solving a nonlinear eigenvalue problem using a phase-plane analysis, following Gratton & Minotti (1990) and Zheng *et al.* (2014). In addition, we have obtained a regime diagram that describes whether the front reaches the origin or not, depending on two dimensionless parameters: r_{out}/r_0 and the drainage constant β. The final location of the front can then be estimated.

We also designed and conducted laboratory experiments for viscous converging gravity currents over a perforated substrate, which serves as a model of continuous leakage, where the flow is generated by removing a cylindrical lock gate within a cylindrical tank. The time evolution of the location of the propagating front was recorded in the experiments, and we observed both flow regimes where the front arrived at the origin and the cases where it did not. The experimental data agree well with the theoretical and numerical predictions. Our experimental set-up provides a new model system for the study of fluid drainage through a thin permeable substrate, and extends the existing experimental systems of drainage through thin parallel plates (Pritchard *et al.* 2001) and drainage through deep substrates (Acton *et al.* 2001; Spannuth *et al.* 2009).

This study can provide useful insights into industrial and geological processes when a liquid fills a crack, for example, in the development of gravity-driven polymer

https://doi.org/10.1017/jfm.2015.406 Published online by Cambridge University Press

crack sealers (e.g. Sprinkel & DeMars 1995) and in the process of crack propagation assisted by chemical reaction (e.g. Atkinson 1984; Vlassak, Lin & Tsui 2005). For these processes, it is useful to understand the dynamics of the fluid motion and the time scale when the fluid front arrives at the crack tip. Here we have analysed the effect of buoyancy-driven fluid loss through a permeable boundary, and how such a drainage effect can alter the crack-filling dynamics. It should also be noted that the effect of surface tension can become important when the propagating front is very close to the crack tip, which forms an interesting topic for future study.

Acknowledgements

We are grateful for the financial support from a grant of the Princeton Environmental Institute at Princeton University. We thank I. Christov, J. Feng, S. Lam, R. Socolow and the anonymous referees for helpful suggestions.

REFERENCES

ACTON, J. M., HUPPERT, H. E. & WORSTER, M. G. 2001 Two-dimensional viscous gravity currents flowing over a deep porous medium. *J. Fluid Mech.* **440**, 359–380.

ATKINSON, B. K. 1984 Subcritical crack growth in geological materials. *J. Geophys. Res.* **89**, 4077–4114.

BARENBLATT, G. I. 1979 *Similarity, Self-Similarity, and Intermediate Asymptotics*. Consultants Bureau.

BEAR, J. 1972 *Dynamics of Fluids in Porous Media*. Elsevier.

CLASS, H. & EBIGBO, A. 2009 A benchmark study on problems related to CO_2 storage in geologic formations. *Comput. Geosci.* **13**, 409–434.

DAGAN, Z., WEINBAUM, S. & PFEFFER, R. 1982 An infinite-series solution for the creeping motion through an orifice of finite length. *J. Fluid Mech.* **115**, 505–523.

DAVIS, S. H. & HOCKING, L. M. 1999 Spreading and imbibition of viscous liquid on a porous base. *Phys. Fluids* **11**, 48–57.

DAVIS, S. H. & HOCKING, L. M. 2000 Spreading and imbibition of viscous liquid on a porous base. II. *Phys. Fluids* **12**, 1646–1655.

DIEZ, J. A., GRATTON, R. & GRATTON, J. 1992 Self-similar solution of the second kind for a convergent viscous gravity current. *Phys. Fluids* A **6**, 1148–1155.

FARCAS, A. & WOODS, A. W. 2009 The effect of drainage on the capillary retention of CO_2 in a layered permeable rock. *J. Fluid Mech.* **618**, 349–359.

GRATTON, J. & MINOTTI, F. 1990 Self-similar viscous gravity currents: phase plane formalism. *J. Fluid Mech.* **210**, 155–182.

HESSE, M. A., TCHELEPI, H. A., CANTWELL, B. J. & ORR, F. M. JR. 2007 Gravity currents in horizontal porous layers: transition from early to late self-similarity. *J. Fluid Mech.* **577**, 363–383.

HESSE, M. A. & WOODS, A. W. 2010 Buoyant disposal of CO_2 during geological storage. *Geophys. Res. Lett.* **37**, L01403.

HUPPERT, H. E. 1982 Flow and instability of a viscous current down a slope. *Nature* **300**, 427–429.

HUPPERT, H. E. & NEUFELD, J. A. 2014 The fluid mechanics of carbon dioxide sequestration. *Annu. Rev. Fluid Mech.* **46**, 255–272.

HUPPERT, H. E. & WOODS, A. W. 1995 Gravity driven flows in porous layers. *J. Fluid Mech.* **292**, 55–69.

JENSEN, K. H., VALENTE, A. X. C. N. & STONE, H. A. 2014 Flow rate through microfilters: influence of the pore size distribution, hydrodynamic interactions, wall slip, and inertia. *Phys. Fluids* **26**, 052004.

LAKE, L. W. 1989 *Enhanced Oil Recovery*. Prentice-Hall.

LISTER, J. R. 1992 Viscous flows down an inclined plane from point and line sources. *J. Fluid Mech.* **242**, 631–653.

https://doi.org/10.1017/jfm.2015.406 Published online by Cambridge University Press

MacMinn, C. W., Szulczewski, M. L. & Juanes, R. 2010 CO_2 migration in saline aquifers. Part 1. Capillary trapping under slope and groundwater flow. *J. Fluid Mech.* **662**, 329–351.

Murray, J. D. 1989 *Mathematical Biology*. Springer.

Neufeld, J. A. & Huppert, H. E. 2009 Modelling carbon dioxide sequestration in layered strata. *J. Fluid Mech.* **625**, 353–370.

Neufeld, J. A., Vella, D. & Huppert, H. E. 2009 The effect of a fissure on storage in a porous medium. *J. Fluid Mech.* **639**, 239–259.

Neufeld, J. A., Vella, D., Huppert, H. E. & Lister, J. R. 2011 Leakage from gravity currents in a porous medium. Part 1. A localized sink. *J. Fluid Mech.* **666**, 391–413.

Nordbotten, J. M. & Celia, M. A. 2006 Similarity solutions for fluid injection into confined aquifers. *J. Fluid Mech.* **561**, 307–327.

Nordbotten, J. M. & Celia, M. A. 2012 *Geological Storage of CO_2*. Wiley.

Nordbotten, J. M., Kavetski, D., Celia, M. A. & Bachu, S. 2009 Model for CO_2 leakage including multiple geological layers and multiple leaky wells. *Environ. Sci. Technol.* **43**, 743–749.

Pegler, S. S., Huppert, H. E. & Neufeld, J. A. 2014*a* Fluid injection into a confined porous layer. *J. Fluid Mech.* **745**, 592–620.

Pegler, S. S., Huppert, H. E. & Neufeld, J. A. 2014*b* Fluid migration between confined aquifers. *J. Fluid Mech.* **757**, 330–353.

Phillips, O. W. 1991 *Flow and Reactions in Porous Rocks*. Cambridge University Press.

Pritchard, D. 2007 Gravity currents over fractured substrates in a porous medium. *J. Fluid Mech.* **584**, 415–431.

Pritchard, D. & Hogg, A. J. 2002 Draining viscous gravity currents in a vertical fracture. *J. Fluid Mech.* **459**, 207–216.

Pritchard, D., Woods, A. W. & Hogg, A. J. 2001 On the slow draining of a gravity current moving through a layered permeable medium. *J. Fluid Mech.* **444**, 23–47.

Sampson, R. A. 1891 On Stokes's current function. *Phil. Trans. R. Soc. Lond.* A **182**, 449–518.

Seminara, A., Angelini, T. E., Wilking, J. N., Vlamakis, H., Ebrahim, S., Kolter, R., Weitz, D. A. & Brenner, M. P. 2012 Osmotic spreading of bacillus subtilis biofilms driven by an extracellular matrix. *Proc. Natl Acad. Sci. USA* **109**, 1116–1121.

Smith, S. H. 1969 On initial value problems for the flow in a thin sheet of viscous liquid. *Z. Angew. Math. Phys.* **20**, 556–560.

Spannuth, M. J., Neufeld, J. A., Wettlaufer, J. S. & Worster, M. G. 2009 Axisymmetric viscous gravity currents flowing over a porous medium. *J. Fluid Mech.* **622**, 135–144.

Sprinkel, M. M. & DeMars, M. 1995 Gravity-fill polymer crack sealers. *Transp. Res. Rec.* **1490**, 43–53.

Vella, D., Neufeld, J. A., Huppert, H. E. & Lister, J. R. 2011 Leakage from gravity currents in a porous medium. Part 2. A line sink. *J. Fluid Mech.* **666**, 414–427.

Vlassak, J. J., Lin, Y. & Tsui, T. Y. 2005 Fracture of organosilicate glass thin films: environmental effects. *Mater. Sci. Engng* A **391**, 159–174.

Weissberg, H. L. 1962 End correction for slow viscous flow through long tubes. *Phys. Fluids* **5**, 1033–1036.

Woods, A. W. & Farcas, A. 2009 Capillary entry pressure and the leakage of gravity currents through a sloping layered permeable rock. *J. Fluid Mech.* **618**, 361–379.

Zemoch, P. J., Neufeld, J. A. & Vella, D. 2011 Leakage from inclined porous reservoirs. *J. Fluid Mech.* **673**, 395–405.

Zheng, Z., Christov, I. C. & Stone, H. A. 2014 Influence of heterogeneity on second-kind self-similar solutions for viscous gravity currents. *J. Fluid Mech.* **747**, 218–246.

Zheng, Z., Guo, B., Christov, I. C., Celia, M. A. & Stone, H. A. 2015 Flow regimes for fluid injection into a confined porous medium. *J. Fluid Mech.* **767**, 881–909.

Zheng, Z., Soh, B., Huppert, H. E. & Stone, H. A. 2013 Fluid drainage from the edge of a porous reservoir. *J. Fluid Mech.* **718**, 558–568.

https://doi.org/10.1017/jfm.2015.406 Published online by Cambridge University Press